

Supplementary information for

Regulation of the macrolide resistance ABC-F translation factor MsrD

**Corentin R. Fostier¹, Farès Ousalem¹, Elodie C. Leroy², Saravuth Ngo¹,
Heddy Soufari^{2,3}, C. Axel Innis², Yaser Hashem^{2,*}, Grégory Boël^{1,4,*}**

¹Expression Génétique Microbienne, CNRS, Université Paris Cité, Institut de Biologie Physico-Chimique, 75005 Paris, France

²INSERM U1212 (ARNA), Institut Européen de Chimie et Biologie, Université de Bordeaux, 33607 Pessac, France

³Current address: NovAliX, Boulevard Sébastien Brant, Bioparc, 67405 Illkirch Cedex, France

⁴Lead contact

*Correspondence:

Grégory Boël, Institut de Biologie Physico-Chimique, 13 rue Pierre et Marie Curie, 75005 Paris, France, tel. : +33 (0) 1 58 41 51 21; e-mail: boel@ibpc.fr

Yaser Hashem, Institut Européen de Chimie et Biologie, Université de Bordeaux, 33607 Pessac, France, tel. : +33 (0) 5 40 00 88 22; e-mail: yaser.hashem@inserm.fr

Supplementary Table 1. Minimum inhibitory concentration (MIC) and half maximal inhibitory concentration (IC₅₀) of *E. coli* DB10 expressing *msrD* variants in presence of erythromycin. See Methods for experimental details. MIC values exceeding control plasmid are shown in bold.

<i>E. coli</i> DB10	Erythromycin	
	MIC (μM)	IC ₅₀ (μM)
pBAD- <i>Control</i>	2	0,179 ± 0,007
pBAD- <i>msrD</i> _{WT}	16	4,592 ± 0,582
pBAD- <i>msrD</i> _{EQ2}	2	0,267 ± 0,027
pBAD- <i>msrD</i> _{E125Q}	4	1,427 ± 0,147
pBAD- <i>msrD</i> _{E434Q}	2	0,342 ± 0,04
pBAD- <i>msrD</i> _{ΔLoop}	2	0,209 ± 0,025
pBAD- <i>msrD</i> _{ΔPTIM}	2	0,295 ± 0,048
pBAD- <i>msrD</i> _{R241A}	16	3,632 ± 0,316
pBAD- <i>msrD</i> _{L242A}	8	1,621 ± 0,152
pBAD- <i>msrD</i> _{H244A}	8	1,492 ± 0,126
pBAD- <i>msrD</i> _{H244W}	4	0,446 ± 0,057

Supplementary Table 2. Cryo-EM data collection and refinement statistics.

	Erythromycin-stalled <i>Escherichia coli</i> 70S ribosome with streptococcal MsrDL nascent chain (PDB 7Q4K, EMD-13805, EMD-13806, EMD-13807, EMD-13808)
Data collection and processing	
Microscope	FEI Talos Arctica (IECB, Pessac, France)
Detector	K2 Summit direct electron detector (Gatan)
Magnification (X)	120,000
Voltage (kV)	200
Electron exposure (e ⁻ /Å ²)	64
Defocus range (μm)	-0.5 to -2.7
Pixel size (Å)	1.2
Symmetry imposed	C1
Initial particle images (no.)	158,200
Final particle images (no.)	62,093
Map resolution (Å)	70S ribosome (EMD-13805): 3 50S subunit (EMD-13806): 2.97 30S subunit Body (EMD-13807): 3.08 30S subunit Head (EMD-13808): 3.3
FSC threshold	0.143
Model building and refinement	
Initial model (PDB code)	6TC3
Model resolution (Å)	2.7
FSC threshold	0.143
Model resolution range (Å)	2.5 – 8.7
Model composition	-
Non-hydrogen atoms	146,618
Protein residues	5,682
RNA bases	4,710

Ligands	173
B-factor (Å ²)	-
Protein (min./max./mean)	31.70/183.09/69.05
Ligands (min./max./mean)	20.00/458.82/75.79
R.m.s. deviations	-
Bond lengths (Å)	0.015
Bond angles (°)	1.648
Validation	-
MolProbity score	1.49
Clashscore	3.83
Poor rotamers (%)	0.63
Ramachandran plot	-
Favored (%)	95.42
Allowed (%)	4.45
Disallowed (%)	0.13

Supplementary Table 3. Strains and plasmids used in this study.

Bacterial strains	References
<i>E. coli</i> DB10 (Derived from <i>E. coli</i> PR7)	1
<i>E. coli</i> K12 MG1655	N/A
Plasmids	References
pBAD-Control (pBAD33)	2
pBAD- <i>msrD</i> _{WT} (pVN50)	2
pBAD- <i>msrD</i> _{EQ2}	This study
pBAD- <i>msrD</i> _{E125Q}	This study
pBAD- <i>msrD</i> _{E434Q}	This study
pBAD- <i>msrD</i> _{ΔLoop}	This study
pBAD- <i>msrD</i> _{ΔPtiM}	This study
pBAD- <i>msrD</i> _{R241A}	This study
pBAD- <i>msrD</i> _{L242A}	This study
pBAD- <i>msrD</i> _{H244A}	This study
pBAD- <i>msrD</i> _{H244W}	This study
pMMB-67EH	3
pMMB-67EH- <i>yfp</i>	This study
pMMBpLlacO-1-67EH- <i>yfp</i>	This study
pMMB- <i>msrDL</i> - <i>msrD</i> ₍₁₋₃₎ : <i>yfp</i>	This study
pMMB- <i>msrDL</i> _(no_ORF) - <i>msrD</i> ₍₁₋₃₎ : <i>yfp</i>	This study
pMMB- <i>msrDL</i> _(no_term) - <i>msrD</i> ₍₁₋₃₎ : <i>yfp</i>	This study
pMMB- <i>msrDL</i> _(Y2A) - <i>msrD</i> ₍₁₋₃₎ : <i>yfp</i>	This study
pMMB- <i>msrDL</i> _(L3A) - <i>msrD</i> ₍₁₋₃₎ : <i>yfp</i>	This study
pMMB- <i>msrDL</i> _(I4A) - <i>msrD</i> ₍₁₋₃₎ : <i>yfp</i>	This study
pMMB- <i>msrDL</i> _(F5A) - <i>msrD</i> ₍₁₋₃₎ : <i>yfp</i>	This study
pMMB- <i>msrDL</i> _(M6A) - <i>msrD</i> ₍₁₋₃₎ : <i>yfp</i>	This study
pMMB- <i>msrDL</i> _(UAA>UGA) - <i>msrD</i> ₍₁₋₃₎ : <i>yfp</i>	This study
pMMB- <i>msrDL</i> _(UAA>UAG) - <i>msrD</i> ₍₁₋₃₎ : <i>yfp</i>	This study
pMMB- <i>msrDL</i> _(WT-isocodons) - <i>msrD</i> ₍₁₋₃₎ : <i>yfp</i>	This study
pMMB- <i>msrDL</i> _(MYLIFMA-isocodons) - <i>msrD</i> ₍₁₋₃₎ : <i>yfp</i>	This study

Supplementary Table 4. Oligonucleotides used in this study.

No.	Name	Sequence (5' → 3')	Purpose
pBAD plasmids			
1	msrD_F	ATGGAATTAATATTTAAAGCAA AAGACATTCGTGTGG	Amplification of <i>msrD</i> _{WT}
2	msrD_R	TTAGTGATGGTGATGGTGATG TTTCAGATTTATTTTCTTATC	
3	pBAD_F	CATCACCATCACCATCACTAAT CTAGAGTCGACCTGCAGGC	Amplification of pBAD backbone
4	pBAD_R	GCTTTTAATATTAATTCATGG TGAATTCCTCCTGCTAGCC	
5	msrD _{EQ2} _F1	GGTATTTTAGCGGATCAACCTA CGAG	<i>msrD</i> mutagenesis
6	msrD _{EQ2} _R1	GGAAGTTACTGGGTTGATCCA TTATTAG	
7	msrD _{EQ2} _F2	AACCCAGTAACTTCCTTGACAT ACC	
8	msrD _{EQ2} _R2	GATCCGCTAAAATACCATGAAC C	
9	msrD _{E125Q} _F	GGTATTTTAGCGGATCAACCTA CGAGCCATTTAG	
10	msrD _{E125Q} _R	GGCTCGTAGGTTGATCCGCTA AAATACCATG	
11	msrD _{E434Q} _F	CTAATAATGGATCAACCCAGTA ACTTCCTTGAC	
12	msrD _{E434Q} _R	GGAAGTTACTGGGTTGATCCA TTATTAGGATG	
13	msrD _{ΔLoop} _F	GGAAAGGGCTGCGGAGGAAA AGGGAGGAGGAAAGATGTATA ATGCTGCTAAAAC	
14	msrD _{ΔLoop} _R	GCAGCATTATACATCTTTCCTC CTCCCTTTTCCTCCGCAGCCC TTTCCAATCGGG	
15	msrD _{ΔPIM} _F	CTGATTATCTTCGTCAGAAAGG AGGAGGACCGGAAGGCATTCTG CAGAATTCG	
16	msrD _{ΔPIM} _R	CGAATTCTGCGAATGCCTTCC GGTCCTCCTCCTTTCTGACGA AGATAATCAGAATAG	
17	msrD _{R241A} _F	GAAGACGGAGGGGCTTTAGCT CATCAAAAATC	
18	msrD _{R241A} _R	GATGAGCTAAAGCCCCTCCGT CTTCAGTAC	
19	msrD _{L242A} _F	GACGGAGGGCGTGCAGCTCAT CAAAAATCAATAG	
20	msrD _{L242A} _R	GATTTTTGATGAGCTGCACGC CCTCCGTCTTCAG	
21	msrD _{H244A} _F	GCGTTTAGCTGCTCAAAAATCA ATAGGAAGTAAGG	

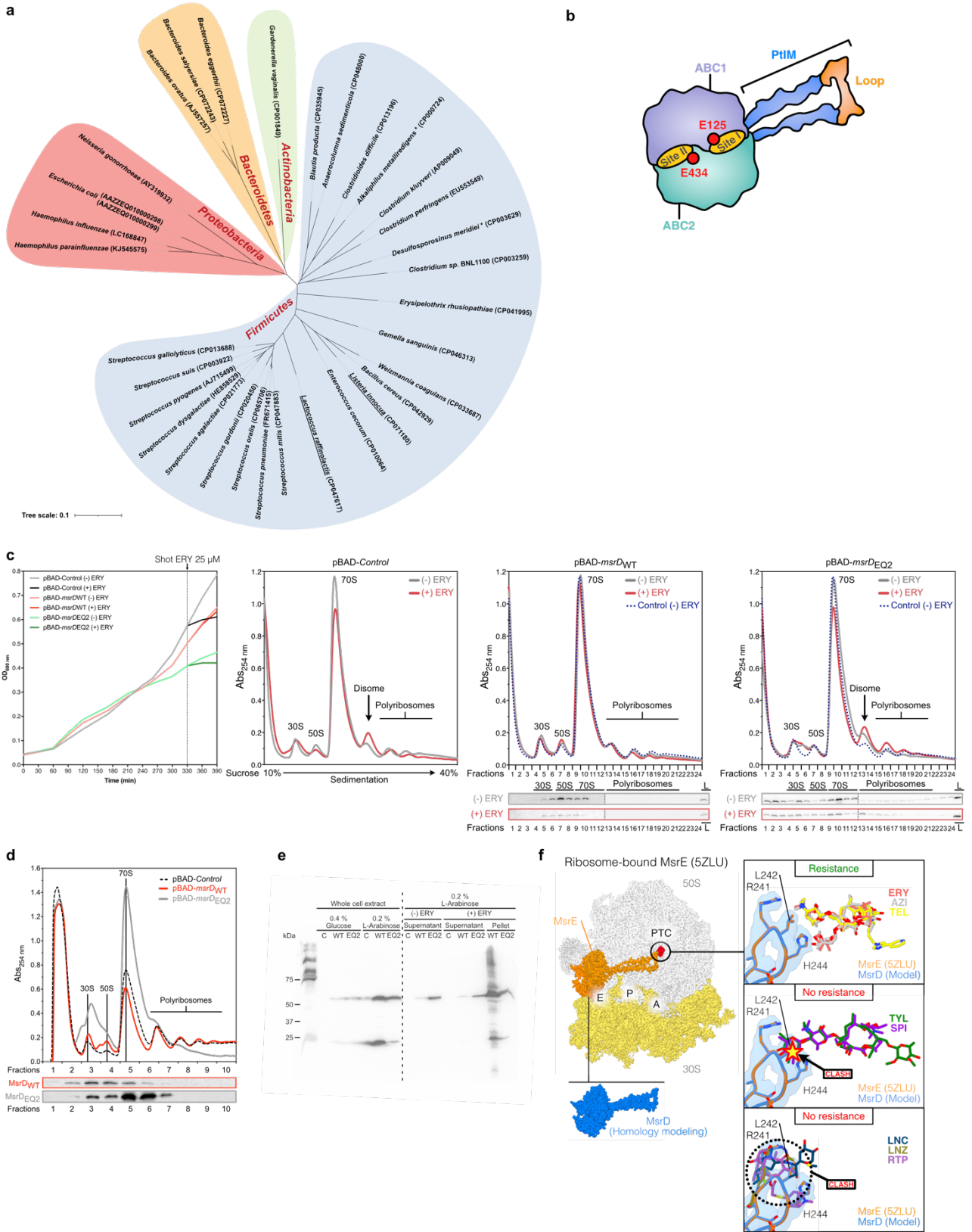
22	msrD _{H244A} _R	CTATTGATTTTTGAGCAGCTAA ACGCCCTCCGTCTTC	
23	msrD _{H244W} _F	GCGTTTAGCTTGGCAAAAATCA ATAGGAAGTAAGG	
24	msrD _{H244W} _R	CTATTGATTTTTGCCAAGCTAA ACGCCCTCCGTCTTC	
pMMB plasmids			
25	pMMB-PlacO_F	GTATAAATGTGAGCGGATAAC ATTGACATTGTGAGCGGATAA CAAGATACTGAGCACATCACA CAGGAAACAGAATATGTCC	Replacement of P _{tac} promoter by P _{lacO} ⁴
26	pMMB-PlacO_R	GTTATCCGCTCACATTTATACA GCTCATTTCAGAATATTTGCC	
27	msrDL-msrD ₍₁₋₃₎ :yfp_F1	CGCAGGGTTTTCCCTGCATAC AAGCAAATGAAAGCATGCGAT TATAGACAGGAGGAAATGTTAT GGAATTAATCGTAAAAATCGTG AGCAAGG	Fusion of <i>msrDL</i> - <i>msrD</i> ₍₁₋₃₎ cistron to <i>yfp</i>
28	msrDL-msrD ₍₁₋₃₎ :yfp_F2	CTGAGCACAACAATATTGGAG GAATATTTATGTATCTTATTTTC ATGTA ACTCTTCTGCTAAAAT CGCAGGGTTTTCCCTGCATAC AAGC	
29	yfp_R	TACTTGTACAGCTCGTCCATG CCGAGAGTGATCCCGGCGGC GG	
30	pMMB-backbone_F	CATGGACGAGCTGTACAAGTA ATAATTCGAGCTCGGTACCCG GG	-
31	pMMB-backbone_R	CCTCCAATATTGTTGTGCTCAG TATCTTGTTATCCGCTCACAAT GTC	-
32	pMMB-control_F	CAACAATATTGGAGGAATATTT TAATTCGAGCTCGGTACCC	-
33	pMMB-control_R	GGGTACCGAGCTCGAATTA ATATTCCTCCAATATTGTTG	-
34	msrDL _(no_term) _F	ATGTATCTTATTTTCATGTA ACTCTCCCTGCATACAAGCAA ATG	Deletion of RIT
35	msrDL _(no_term) _R	AGAGTTACATGAAAATAAGATA CATAAATATTCCTCC	
36	msrDL _(no_ORF) _F	CAACAATATTGGAGGAATATTT TAGTATCTTATTTTCATGTA ACTCTTCC	Suppression of ORF <i>msrDL</i>
37	msrDL _(no_ORF) _R	GGAAGAGTTACATGAAAATA GATACTAAAATATTCCTCCA ATATTGTTG	
38	msrDL _{Y2A} _F	CAATATTGGAGGAATATTTATG GCACTTATTTTCATGTA ACTCTTCC	<i>msrDL</i> mutagenesis
39	msrDL _{Y2A} _R	GGAAGAGTTACATGAAAATA GTGCCATAAATATTCCTCCA ATTTG	
40	msrDL _{L3A} _F	TTGGAGGAATATTTATGTATGC AATTTTCATGTA ACTCTTCC	

41	msrDL _{L3A} _R	GGAAGAGTTACATGAAAATTG CATACATAAATATTCCTCCAA	
42	msrDL _{I4A} _F	GGAGGAATATTTATGTATCTTG CATTCATGTAACCTTCCTG	
43	msrDL _{I4A} _R	CAGGAAGAGTTACATGAATGC AAGATACATAAATATTCCTCC	
44	msrDL _{F5A} _F	GGAATATTTATGTATCTTATTG CAATGTAACCTTCCTG	
45	msrDL _{F5A} _R	CAGGAAGAGTTACATTGCAATA AGATACATAAATATTC	
46	msrDL _{M6A} _F	ATTTATGTATCTTATTTTCGCAT AACTCTTCCTGCTAAAATCGCA GG	
47	msrDL _{M6A} _R	CCTGCGATTTTAGCAGGAAGA GTTATGCGAAAATAAGATACAT AAAT	
48	msrDL _{TAG} _F	GTATCTTATTTTCATGTAGCTC TTCCTGCTAAAATCG	
49	msrDL _{TAG} _R	CGATTTTAGCAGGAAGAGCTA CATGAAAATAAGATAC	
50	msrDL _{TGA} _F	GTATCTTATTTTCATGTGACTC TTCCTGCTAAAATCG	
51	msrDL _{TGA} _R	CGATTTTAGCAGGAAGAGTCA CATGAAAATAAGATAC	
52	msrDL _{MYLIFMA⁻ isocodons} _F	ATGTACCTGATCTTCATGGCCT AACTCTTCCTGCTAAAATCGCA GGG	
53	msrDL _{MYLIFMA⁻ isocodons} _R	TTAGGCCATGAAGATCAGGTA CATAAATATTCCTCCAATATTG TTGTGCTCAGTATCTTGTTATC CGC	
54	msrDL _{WT-isocodons} _F	ATTTATGTACCTGATCTTCATG TAACTCTTCCTGCTAAAATCGC	
55	msrDL _{WT-isocodons} _R	GCGATTTTAGCAGGAAGAGTT ACATGAAGATCAGGTACATAAA T	
In vitro transcription and translation			
56	T7_pMMB_F	GCGAATTAATACGACTCACTAT AGGGAGCGGATAACAAGATAC TGAGCAC	-
57	TP_msrDL_R	GGTTATAATGAATTTTGCTTAT TTAATTCATAACATTTCTCC	-
58	TP_NV1_R	GGTTATAATGAATTTTGCTTAT T	CY5 chromophore modification in 5'
Northern blot probe			
59	pMMB_3UTR	CAGCCAAGCTTGCATGCCTGC AGGTCGACTCTAGAGGATCCC CGGG	-
Cryo-EM			
60	cryoEM-msrDL_R	GCAGGGAAAACCCTGCG	-

Supplementary Table 5. DNA templates used in this study.

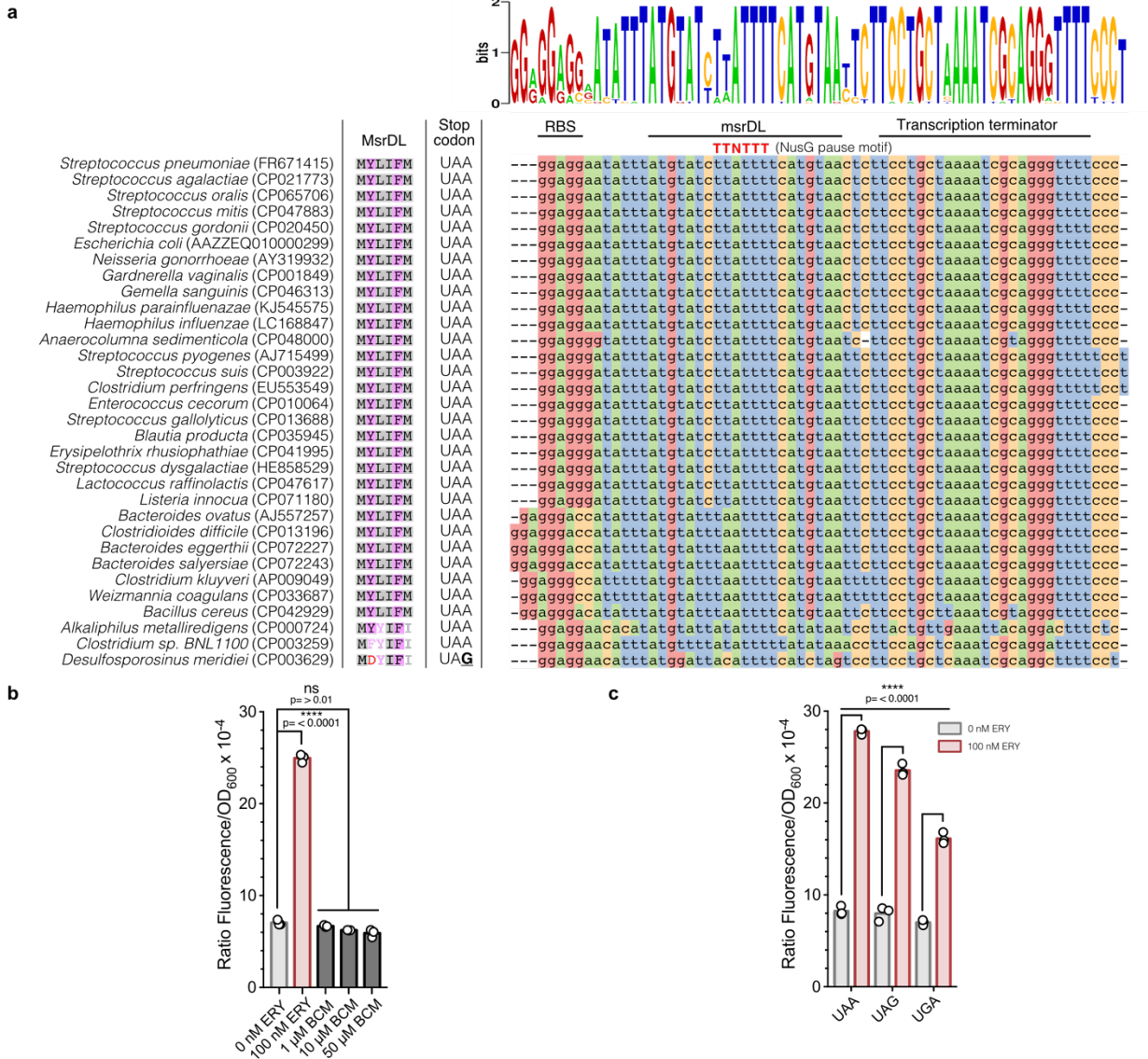
No.	Name	Sequence (5' → 3')
1	TP_msrDL _{WT}	GCGAATTAATACGACTCACTATAGGGAGCGGATAACAAGA TACTGAGCACAAACAATATTGGAGGAATATTTATGTATCTTA TTTTCATGTAACCTCTTCCTGCTAAAATCGCAGGGTTTTCCC TGCATACAAGCAAATGAAAGCATGCGATTATAGACAGGAG GAAATGTTATGGAATTAATAAGCAAATTCATTATAACC
2	TP_msrDL _{7A-iso}	GCGAATTAATACGACTCACTATAGGGAGCGGATAACAAGA TACTGAGCACAAACAATATTGGAGGAATATTTATGTACCTGA TCTTCATGGCCTAACTCTTCCTGCTAAAATCGCAGGGTTTT CCCTGCATACAAGCAAATGAAAGCATGCGATTATAGACAG GAGGAAATGTTATGGAATTAATAAGCAAATTCATTATAA CC
3	CryoEM_msrDL	GCGAATTAATACGACTCACTATAGGGAGCGGATAACAAGA TACTGAGCACAAACAATATTGGAGGAATATTTATGTATCTTA TTTTCATGTAACCTCTTCCTGCTAAAATCGCAGGGTTTTCCC TGC

SUPPLEMENTARY FIGURE 1



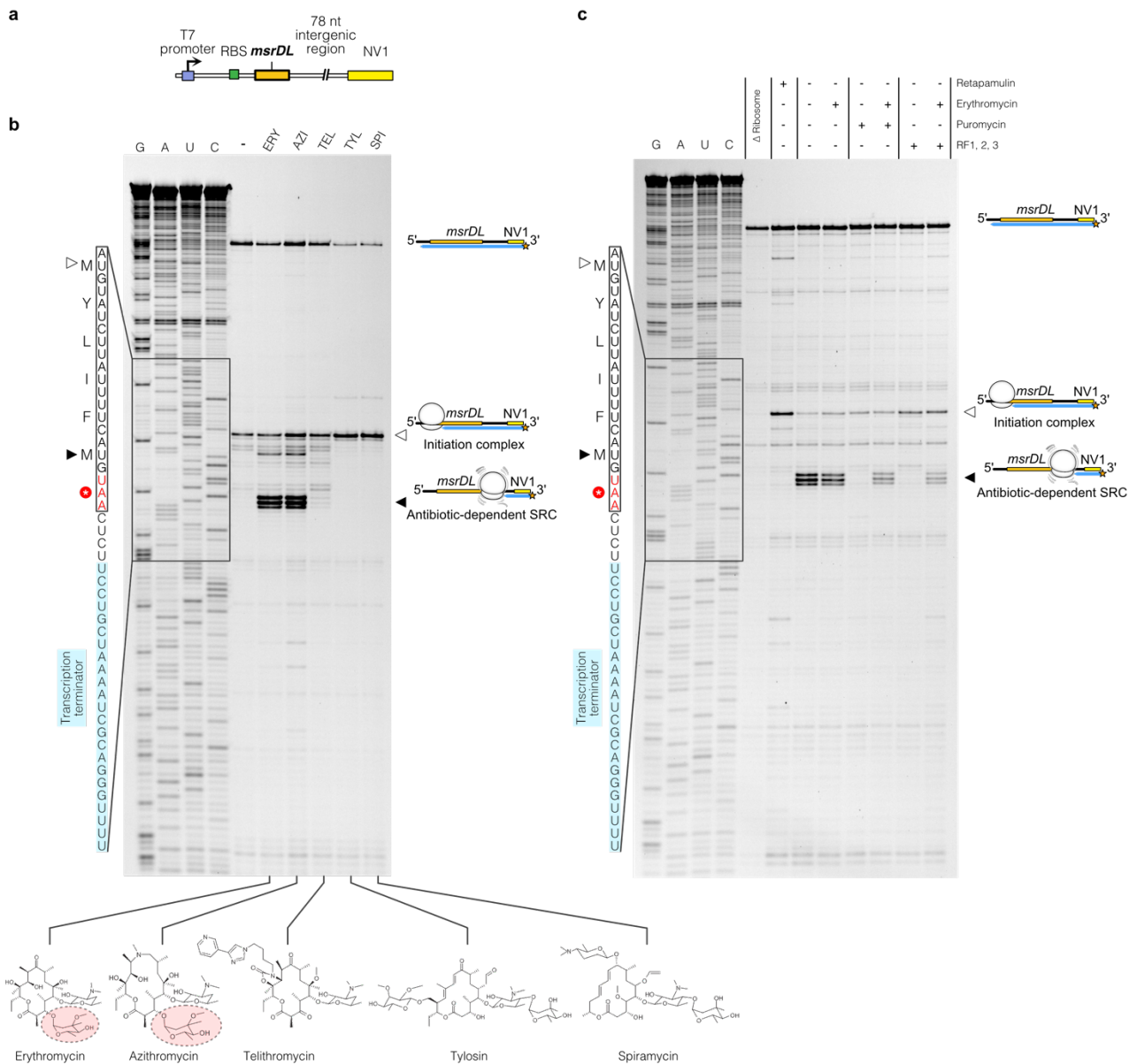
Supplementary figure 1. *In vivo* characterization of MsrD. (a) Dissemination of the *mefA/msrD* macrolide resistance operon among a wide range of non-pathogenic and pathogenic bacterial species. The *mefA/msrD* operon (Genbank accession No. FR671415) was blasted and identified in indicated species, integrated to the genome. Species where the operon was found on plasmid are underlined. Species where *msrD* was found to disseminate alone with *msrDL* are indicated by an asterisk. Corresponding Genebank accession numbers are indicated between brackets. To generate the tree, 16S rRNA sequences were retrieved, aligned using Clustal W⁵, and resulting cladogram was adapted on iTOL (<https://itol.embl.de/>). Colored zones indicate bacterial phyla. (b) Schematic of MsrD illustrating main features of ABC-F translation factors and the position of ATP hydrolysis Site I and Site II whose catalytic residues are respectively E125 and E434. Colors are the same as Fig. 1b. (c) Growth curves, polyribosomes analysis and western blotting of *E. coli* DB10 strain expressing *msrD* (pBAD-*msrD*_{WT}), *msrD*_{EQ2} (pBAD-*msrD*_{EQ2}) or a control (pBAD-*Control*) unexposed or exposed to 25 μM of ERY during one hour (Cells were treated after 330 min as indicated by “Shot ERY 25 μM”). “L” stands for total lysate. Note that these sample were precipitated with trichloroacetic acid (d) Polyribosomes analysis and western-blotting of *E. coli* K12 MG1655 expressing *msrD*_{WT} (pBAD-*msrD*_{WT}), *msrD*_{EQ2} (pBAD-*msrD*_{EQ2}) or a control (pBAD-*Control*). As no erythromycin was added, 100 μg.ml⁻¹ chloramphenicol was added to stabilize translating ribosomes. (e) Solubility assay shows that MsrD_{WT} tends precipitate in insoluble fraction while MsrD_{EQ2} tends to stay more soluble. *E. coli* DB10 strain containing pBAD-*Control* (“C”), pBAD-*msrD*_{WT} (WT) or pBAD-*msrD*_{EQ2} (“EQ2”) was inoculated at OD₆₀₀=0.1 and grew in presence of 0.4 % Glucose or 0.2 % L-Arabinose at 37 °C under vigorous shaking for 6 hours. Cultures were normalized, centrifuged and resuspended (1 ml at OD₆₀₀=1 was resuspended in 30 μL Laemmli 1X). In total, 5 μL of whole cell extract were loaded on SDS-PAGE gel. In parallel, cultures similar to those realized for polyribosome analysis presented in Fig. 1c and 1d were done. Briefly, cells were inoculated at OD₆₀₀=0.1 and grew in presence of 0.2 % L-Arabinose at 37 °C under vigorous shaking. During mid-exponential phase, 25 μM ERY was added or not. Cells were harvested and lysed after 1 h, lysate being clarified by centrifugation from insoluble fraction. After normalization of lysate, a total of 10 μg of RNAs were load on SDS-PAGE gel. Western-blotting was performed as explained in Methods. (f) Steric occlusion mechanism by MsrD is incompatible with its resistance profile. A homology model of MsrD was generated using SWISS-MODEL⁶ and aligned to ribosome-bound MsrE structure (PDB 5ZLU)⁷. Antibiotics to which MsrD provides resistance (ERY PDB: 6ND6, red; AZI PDB: 4V7Y, gray; TEL PDB: 4V7Z, yellow) or not (TYL PDB: 1K9M, green; SPI PDB: 1KD1, violet; LNC PDB: 5HKV, dark teal; LNZ PDB: 3CPW, khaki; RTP PDB: 2OGO, purple) were aligned based on domain V of 23S rRNA⁸⁻¹³. Density for MsrE is shown in pale blue, and conserved residues R241A, L242A and H244A are indicated.

SUPPLEMENTARY FIGURE 2



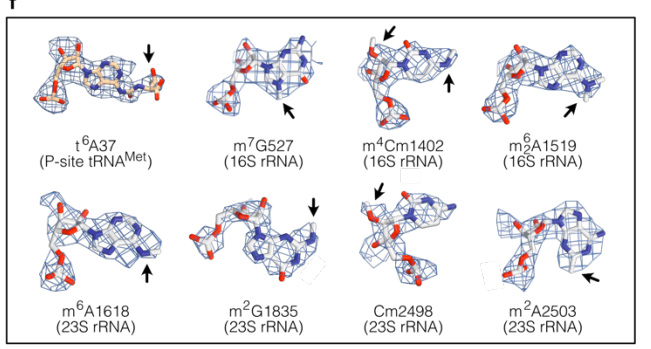
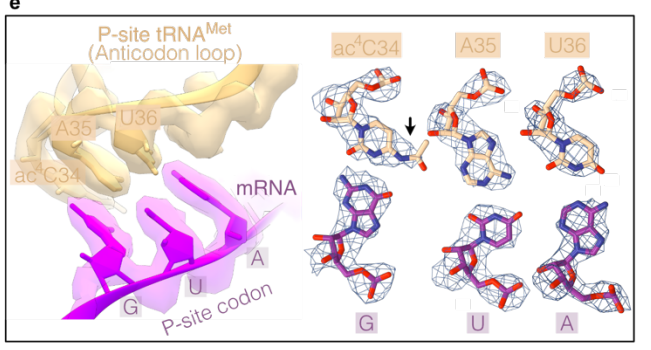
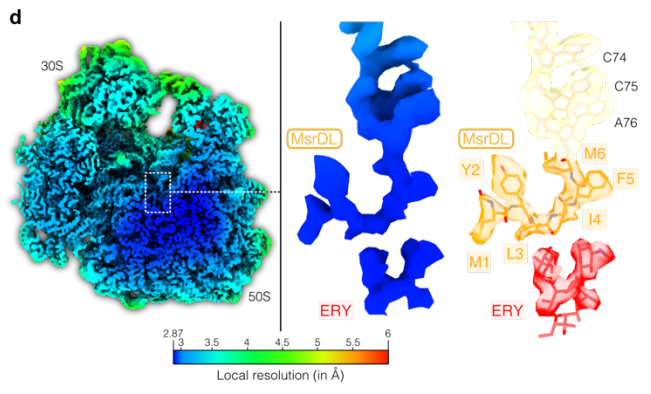
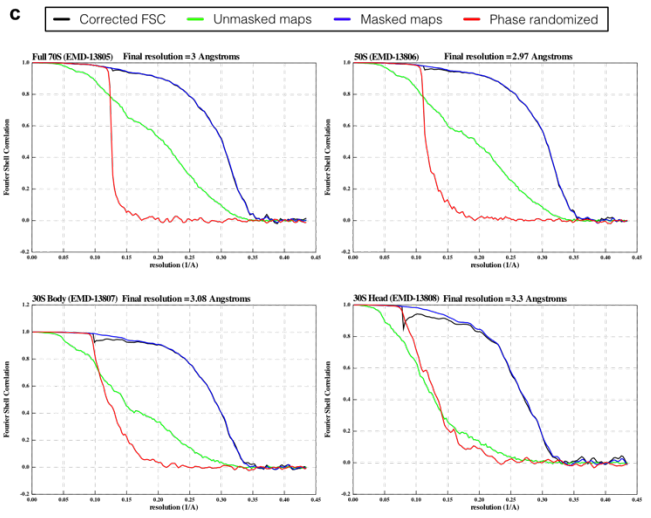
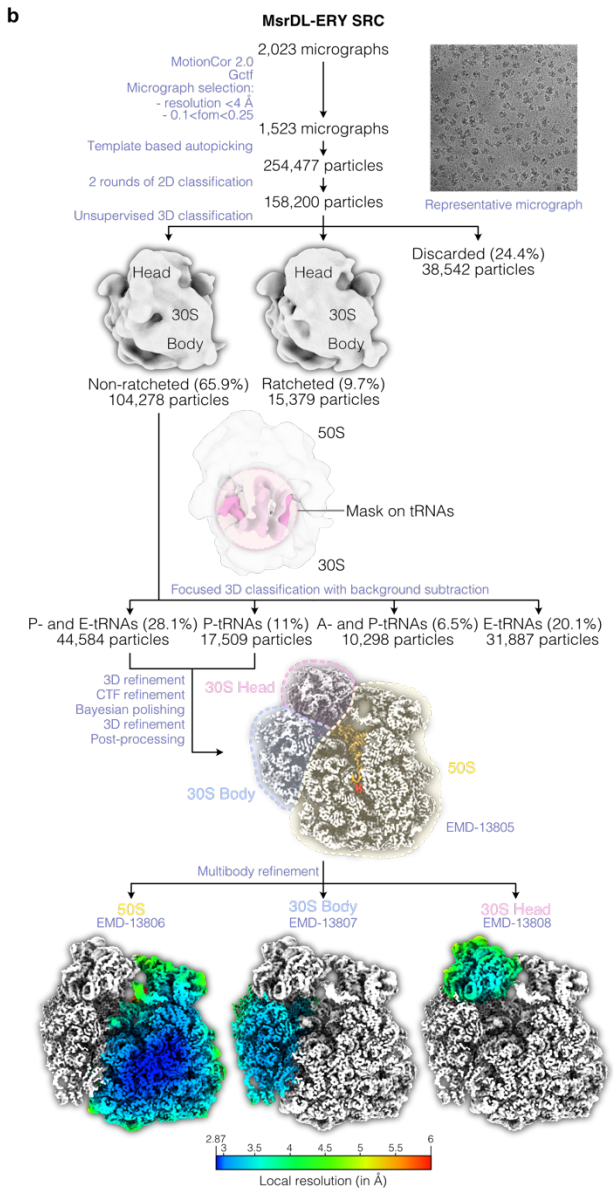
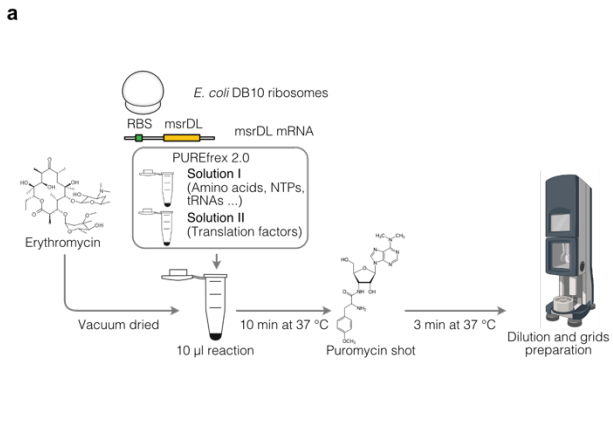
Supplementary figure 2. Rho-independent transcription termination regulates *msrD* expression. (a) Conservation of *msrDL*, NusG-dependent RNAP pausing site and its rho-independent transcription terminator. Sequences corresponding to Fig. 1a were aligned with Clustal W⁵, and visualized with JalView according to nucleotide¹⁴. Genbank accession numbers are indicated between brackets. Logo was generated using WebLogo (<https://weblogo.berkeley.edu/logo.cgi>). (b) Bicyclomycin (BCM) failed to constitutively induce *msrD*₍₁₋₃₎:*yfp* expression in absence of ERY after 17 h, demonstrating that *msrD* is not regulated by a Rho-dependent terminator. Error bars represent mean ± s.d. for triplicate experiments. (c) Effects of *msrDL* stop codon mutation on the expression of *msrD*₍₁₋₃₎:*yfp*. Bacteria were grown during 17 h in presence of 1 mM IPTG, in the absence (grey histograms) or in the presence of 100 nM ERY (red histograms). Error bars represent mean ± s.d. for triplicate experiments.

SUPPLEMENTARY FIGURE 3



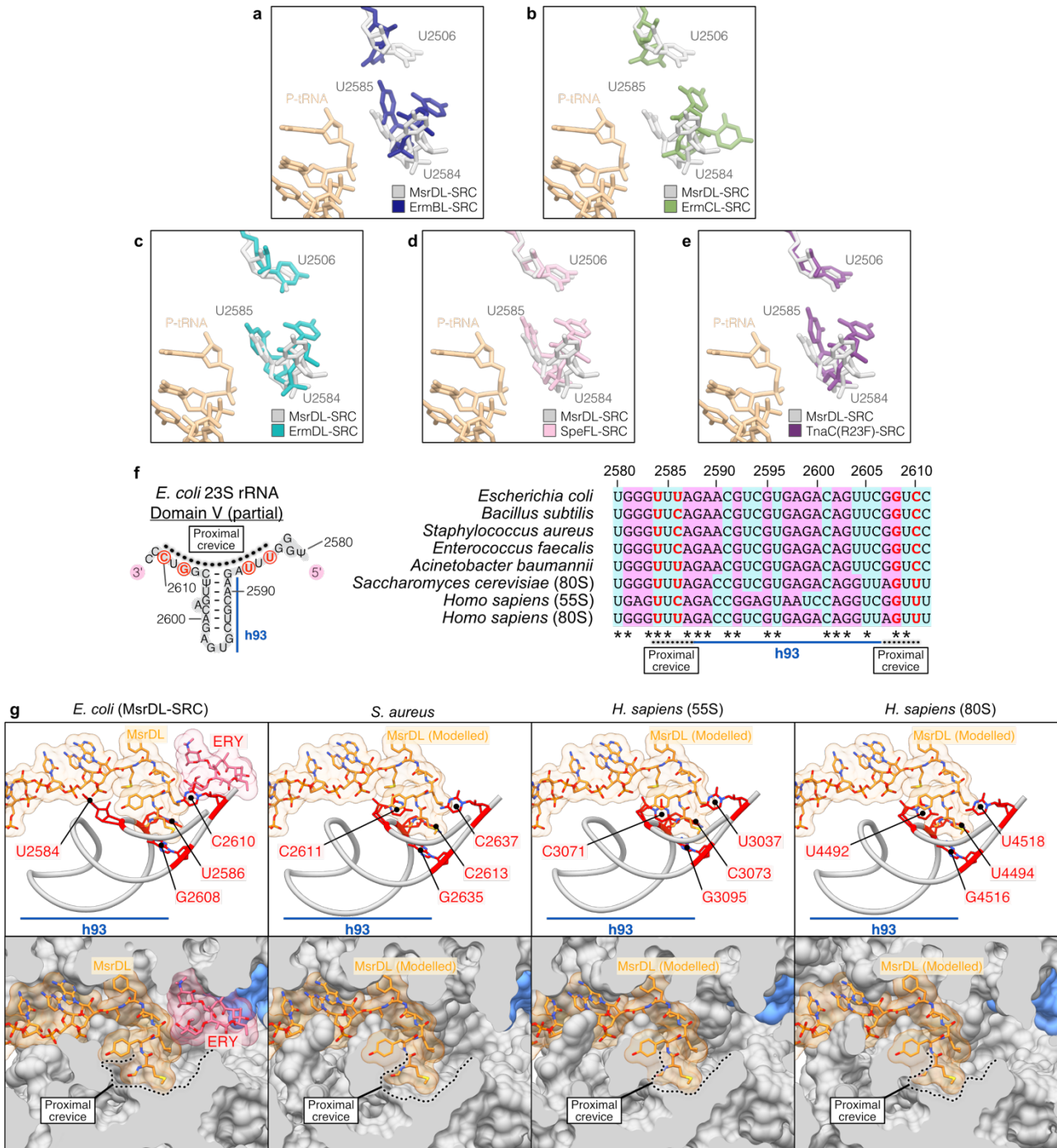
Supplementary figure 3. Biochemical characterization of MsrDL mode of action. (a) Schematic of the matrix TP_msrDL_{WT} (Supplementary Table 5) used to generate synthetic mRNAs for *in vitro* experiments (RBS, ribosome binding site; NV1, annealing site for CY5-labelled primer). (b and c) Uncropped toe-printing gels presented in Fig. 3a and 3c. Formation of MsrDL-SRC would occlude formation of the Rho-independent transcription terminator (shown in light blue).

SUPPLEMENTARY FIGURE 4



Supplementary figure 4. Generation of the cryo-EM sample, data processing and model building. (a) Workflow for the generation of cryo-EM sample. See Methods for details. (b) Cryo-EM data processing workflow as described in the Methods. EMD accession numbers are indicated for each map. Maps obtained after multibody refinement are shown as transverse sections and colored according to local resolution. (c) Fourier Shell Correlation (FSC) curves of the 70S ribosome and the maps obtained after multibody refinement. (d) Transverse section of the composite map obtained after multibody refinement and isolated densities for MsrDL-tRNA and ERY, colored according to local resolution. The corresponding atomic reconstruction of the nascent chain is shown beside. (e) Details of the mRNA codon-tRNA anticodon interactions and corresponding densities for each nucleotide. (f) Details of clearly identifiable post-transcriptional modifications and corresponding densities.

SUPPLEMENTARY FIGURE 5



Supplementary figure 5. MsrDL engages within a universally conserved crevice at the NPET entrance. (a to e) Comparison of the conformation of 23S rRNA bases U2506, U2584 and U2585 for MsrDL-, ErmBL-, ErmCL-, ErmDL-, SpeFL- and TnaC(R23F)-stalled ribosomes structures^{15–19} (respectively PDB: 5JTE, 3J7Z, 7NSO, 6TC3, 7O1A). Structures were aligned based on domain V of 23S rRNA. (f) Sequence conservation of the proximal crevice between far-related species. The diagram shows a part of 23S rRNA domain V of *E. coli* and the location of proximal crevice at the base of h93. Large subunit rRNAs were aligned using Clustal W⁵

and visualized with Jalview ¹⁴ (purines, purple; pyrimidines, teal). Bases delimitating the proximal crevice (U2584, U2586, G2608 and C2610) are highlighted in red. Nucleotides numbering is relative to *E. coli* 23S rRNA sequence. (g) Structural conservation of the proximal crevice between far-related species. Top, cartoon representation of h93 and proximal crevice in *E. coli*, *S. aureus*, *H. sapiens* 55S mitoribosome and 80S cytosolic ribosome ²⁰⁻²² (respectively PDB: 6YEF, 7A5F, 6OLI). Bases delimitating the proximal crevice are highlighted in red and numbered relative to the considered specie. Bottom, sagittal cut of ribosome tunnel shown on top panels depicted as surface. Ribosomal protein uL4 is shown in pale blue. Structures were aligned based on domain V of 23S rRNA.

SUPPLEMENTARY REFERENCES

1. Datta, N., Hedges, R. W., Becker, D. & Davies, J. Plasmid-determined Fusidic Acid Resistance in the Enterobacteriaceae. *Microbiology*, **83**, 191–196 (1974).
2. Nunez-Samudio, V. & Chesneau, O. Functional interplay between the ATP binding cassette Msr(D) protein and the membrane facilitator superfamily Mef(E) transporter for macrolide resistance in *Escherichia coli*. *Research in Microbiology* **164**, 226–235 (2013).
3. Fürste, J. P. *et al.* Molecular cloning of the plasmid RP4 primase region in a multi-host-range tacP expression vector. *Gene* **48**, 119–131 (1986).
4. Lutz, R. & Bujard, H. Independent and Tight Regulation of Transcriptional Units in *Escherichia coli* Via the LacR/O, the TetR/O and AraC/I1-I2 Regulatory Elements. *Nucleic Acids Res* **25**, 1203–1210 (1997).
5. Larkin, M. A. *et al.* Clustal W and Clustal X version 2.0. *Bioinformatics* **23**, 2947–2948 (2007).
6. Waterhouse, A. *et al.* SWISS-MODEL: homology modelling of protein structures and complexes. *Nucleic Acids Res* **46**, W296–W303 (2018).
7. Su, W. *et al.* Ribosome protection by antibiotic resistance ATP-binding cassette protein. *PNAS* **115**, 5157–5162 (2018).
8. Bulkley, D., Innis, C. A., Blaha, G. & Steitz, T. A. Revisiting the structures of several antibiotics bound to the bacterial ribosome. *PNAS* **107**, 17158–17163 (2010).
9. Davidovich, C. *et al.* Induced-fit tightens pleuromutilins binding to ribosomes and remote interactions enable their selectivity. *PNAS* **104**, 4291–4296 (2007).
10. Hansen, J. L. *et al.* The Structures of Four Macrolide Antibiotics Bound to the Large Ribosomal Subunit. *Molecular Cell* **10**, 117–128 (2002).
11. Ippolito, J. A. *et al.* Crystal Structure of the Oxazolidinone Antibiotic Linezolid Bound to the 50S Ribosomal Subunit. *J. Med. Chem.* **51**, 3353–3356 (2008).
12. Matzov, D. *et al.* Structural insights of lincosamides targeting the ribosome of *Staphylococcus aureus*. *Nucleic Acids Research* **45**, 10284–10292 (2017).
13. Svetlov, M. S. *et al.* High-resolution crystal structures of ribosome-bound chloramphenicol and erythromycin provide the ultimate basis for their competition. *RNA* **25**, 600–606 (2019).
14. Waterhouse, A. M., Procter, J. B., Martin, D. M. A., Clamp, M. & Barton, G. J. Jalview Version 2—a multiple sequence alignment editor and analysis workbench. *Bioinformatics* **25**, 1189–1191 (2009).
15. Arenz, S. *et al.* Drug Sensing by the Ribosome Induces Translational Arrest via Active Site Perturbation. *Molecular Cell* **56**, 446–452 (2014).
16. Arenz, S. *et al.* A combined cryo-EM and molecular dynamics approach reveals the mechanism of ErmBL-mediated translation arrest. *Nat Commun* **7**, (2016).
17. Beckert, B. *et al.* Structural and mechanistic basis for translation inhibition by macrolide and ketolide antibiotics. *Nat Commun* **12**, 4466 (2021).
18. Herrero del Valle, A. *et al.* Ornithine capture by a translating ribosome controls bacterial polyamine synthesis. *Nature Microbiology* **5**, 554–561 (2020).
19. van der Stel, A.-X. *et al.* Structural basis for the tryptophan sensitivity of TnaC-mediated ribosome stalling. *Nat Commun* **12**, 5340 (2021).
20. Desai, N. *et al.* Elongational stalling activates mitoribosome-associated quality control. *Science* **370**, 1105–1110 (2020).
21. Golubev, A. *et al.* Cryo-EM structure of the ribosome functional complex of the human pathogen *Staphylococcus aureus* at 3.2 Å resolution. *FEBS Letters* **594**, 3551–3567 (2020).
22. Li, W. *et al.* Structural basis for selective stalling of human ribosome nascent chain complexes by a drug-like molecule. *Nat Struct Mol Biol* **26**, 501–509 (2019).